2020 Building Performance Analysis Conference and
SimBuild co-organized by ASHRAE and IBPSA-USA

EVALUATION OF RAMMED EARTH ASSEMBLIES AS THERMAL MASS THROUGH WHOLE-BUILDING SIMULATION

Pragya Gupta[1], Dana Cupkova[1], Lola Ben-Alon[1], and Erica Cochran Hameen[1]
[1]School of Architecture, Carnegie Mellon University, Pittsburgh, PA

ABSTRACT

Rammed earth is a low-carbon and nontoxic alternative to conventional construction materials. It was shown to be beneficial in hot climates, making it prominent for resiliency in the face of climate change. However, rammed earth is not broadly implemented due to its low thermal resistance, even though many studies have elaborated the benefits through its mass, specific heat capacity and hygroscopic properties. This paper presents a comparative thermal simulation of rammed earth and mainstream concrete and wood assemblies, accounting for both heat resistivity and capacity. Rammed earth is shown to provide a steady-state indoor temperature levels while decreasing heating and cooling loads in 20%-52% as opposed to conventional assemblies.

INTRODUCTION

Buildings contribute to approximately a third of the world's final energy use. Space heating and cooling account for approximately 35% of the total operational emissions of buildings while another 11% is emitted due to construction (UN Environmental and International Energy Agency, 2017) (Perez-Lombard, Ortiz, & Pout, 2008). With such a staggering impact on global energy consumption and greenhouse gas emissions, it is imperative that we find solutions that would minimize the energy requirements over the entire lifecycle of the building – construction, operation and demolition.

Rammed earth construction was shown to be an environmentally benign alternative to current construction materials (Cabeza, et al., 2013). It utilizes locally sourced materials, requires minimal processing, and is a healthy, non-toxic material providing enhanced indoor air quality (Treloar, Owen, & Fay, 2001). Rammed earth has high density 96.14 lb/ft^3 (1,540 kg/m^3) and extremely high specific heat capacity 300.94 BTU/lb·°F (1,260 J/kg·K) (Hugo & Guillaud, 1984) (AIRAH, 2000). Combined with low resistivity (CSIRO, 2000) (Taylor & Luther, 2004), rammed earth is ideal for thermal mass construction and application (Gilly, 1787). In addition, rammed earth was shown to be especially beneficial in high diurnal temperature ranges (Hall & Djerbib, 2006), where it was shown to be able to both moderate indoor temperatures and shift the peak temperatures (Minke, 2006). For instance, Soudani, et al. (2016) show a 6-9-hour time lag in continental climates and measured a 46-48°F (8-9°C) temperature difference that considerably reduced the load on mechanical systems (Soudani, Woloszyn, Fabbri, Morel, & Grillet, 2017). In another study, a 10-hour shift in peak temperature was measured with about 25% reduction in amplitude of heat flux on the inner wall surface (Taylor & Luther, 2004). In a multi-city comparative study in Egypt, as much as 40% energy savings was reported when rammed earth was used in place of hollow cement block in the west wall. The study also found that 12" (30 cm) rammed earth wall was the most optimum thickness for Egypt (Hatem & Karram, 2016).

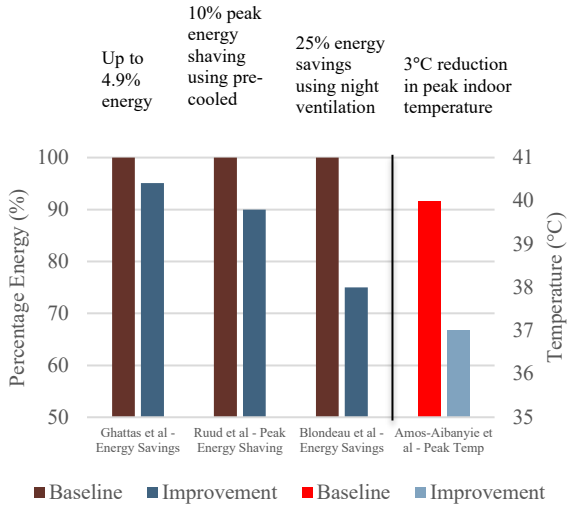

Figure 1 Comparison of simulation studies for thermal mass performance.

Figure 1 summarizes the various simulation studies that account for thermal mass properties (Ghattas, Ulm, & Ledwith, 2013) (Ruud, Mitchell, & Klein, 1990)

(Blondeau, Sperandio, & Allard, 1997) and (Amos-Abanyie & Akuffo, 2013) showing that it can both reduce the heating and cooling load and contribute in shifting peak demand.

Another key benefit of rammed earth is its ability to regulate humidity. It was observed that stabilized rammed earth walls can maintain relative humidity levels of 50-60% as compared to painted plasterboard that results in humidity fluctuation between 40-85%. This reduces the energy consumption for humidification and dehumidification (Allinson & Hall, 2010).

While these studies show the significant impacts of thermal mass on achieving comfort conditions, very few offer a comprehensive comparison of various thicknesses of rammed earth, location of insulation within the assembly and its comparison with mainstream construction assemblies. Therefore, this study aims to provide a comparative evaluation of prevalent construction assemblies and high-performance rammed earth assembly for additional locations and climate zones to better address material selection over a range of climates and cities. Additionally, this study investigates the impact of rammed earth wall thickness and insulation location on the annual heating and cooling loads. Lastly, indoor air temperature profiles and surface temperature fluctuations are analyzed to compare the performance of each assembly with respect to the sinusoidal outdoor temperature variation.

This study is conducted in two phases. In the first phase, multiple rammed earth assemblies are simulated using a whole-building simulation to measure the impacts of earthen thermal mass and the location of the insulation layer on heating and cooling loads. The highest performing assembly is then compared to prevalent construction assemblies – cavity brick construction, insulated wood frame, and insulated concrete in four cities: Bishkek (Kyrgyzstan), Jaipur (India), Lanzhou (China), and Tehran (Iran).

METHODOLOGY AND MODEL PARAMETERS

The comparative study is performed using an energy simulation model developed in DesignBuilder v.6 (DesignBuilder, 2019), a graphical user interface for EnergyPlus (Energy, 2019) simulation engine. The main aim of the study was to investigate the thermal performance and energy impacts of earthen mass construction. To achieve this goal, the study includes the following steps:

1. Gathering data on rammed earth assemblies including materials physics and thermal performance.

2. Assessing the climatic conditions of the simulated locations and their suitability for earthen construction.

3. Investigating the impacts of various rammed earth wall thicknesses and locations of an additional insulation layer.

4. Comparison of rammed earth assembly and selected mainstream construction assemblies with respect to heating and cooling load profiles.

As shown in Table 1, four different cities were selected due to their climatic context and traditional use of earthen materials.

Table 1 Overview of cities selected for simulation

Location	Koppen Climate classification (Beck, et al., 2018) TemperatureRange	Prevalent traditional earthen construction
Bishkek, Kyrgyzstan	Dsa – Hot Summer Continental Climate 98–10°F (37- -12°C)	Adobe (Uranova & Begaliev, 2002)
Jaipur, India	Bsh – Hot Desert Climate 112–40°F (44-4°C)	Cob, Adobe, Sandstone (Rathore, Sharma, & Preet, 2018)
Lanzhou, China	Bsk – Semi-Arid Climate 98 – 0°F (37- -18°C)	Rammed Earth (Li, et al., 2011)
Tehran, Iran	Csa – Hot Summer Mediterranean Climate 100–24°F (38- -4°C)	Earthen Domes (Sabzi, 2018)

A typical residential building was modeled with a floor area of 2,752 ft^2 (256 m^2) and occupied volume of 16,406 ft^3 (465 m^3). The building layout was developed as per the DOE prototype (Kneifel, 2012).

The Finite Difference algorithm that uses fundamental calculation formation was used rather than the default conduction transfer method due to its suitability to mass materials and better heat transfer calculation fidelity (EnergyPlus, 2019). Fully implicit order based on Adams-Moulton solution (EnergyPlus, 2019) was selected as the calculation scheme for Finite Difference algorithm over the semi-implicit Crank-Nicholson scheme (EnergyPlus, 2019). In this model, the surface discretization accounts for the thermal diffusivity of each material as well as the selected simulation time step rate. A time step of 30 steps per hour was selected to improve the calculation accuracy of the algorithm.

Typical Meteorological Year version 3 (TMY30) weather files (Wilcox & Marion, 2008) were used for simulating all four cities. The internal heat gains included occupancy of 4 people. An ideal load profile was selected for the heating and cooling systems. The model and occupancy parameters, as detailed in Table 2, were kept constant with only the external wall assembly being modified. The various wall assemblies are detailed in Table 3.

Table 2 Simulation Model Parameters - Constant Inputs

Parameter	Selection
Number of Occupants	4
Occupancy Schedule	NIST Residential Occupancy
Activity	Reading Seated
Metabolic Factor	1.0
Clothing Schedule Definition	Generic Summer and Winter Clothing
Calculation Type	Zone Averaged
Environmental Control	
Heating Setpoint	68 °F (20 °C) (ASHRAE, 2010)
Cooling Setpoint	76 °F (24 °C) (ASHRAE, 2010)
Minimum Fresh Air Rate	5.297 ft^3/min-person
Mechanical Vent per Area	0.059 ft^3/min-ft^2
Construction Assemblies	
Below Grade Walls	4 in Brick + 4 in XPS + 4 in CMU + 0.5 in Gypsum Plastering
Flat Roof	0.75 in Asphalt + 4 in Fiberboard + 2 in XPS + 4 in Cast Concrete
Pitched Roof (Occupied)	1 in Clay Tile + 4 in Stone Wool + 0.2 in roofing Felt
Pitched Roof (Unoccupied)	1 in Clay Tile + 4 in Stone Wool + 0.2 in roofing Felt
Ground Floor	4 in Foam + 4 in Cast Concrete + 2.75 in Screed + 1.2 in Timber Flooring
External Floor	1 in External Rendering + 4 in Stone Wool + 0.2 in Timber Flooring
Airtightness rate	0.3 ac/h, 24/7
Window to Wall Ratio	15%
Glazing Type	Double Pane Clear Reflective Glass with 6mm Air Gap
Frame	Aluminum Window Frames (with thermal break)
Shading	Blinds with highly reflective slats
Control Type	Inside Air Temperature
HVAC Options	
HVAC Template	Ideal Loads
Heating System	Gas Furnace, Available 24/7
Cooling System	Air Conditioner, Available 24/7

The internally insulated Rammed Earth assembly was composed of 4in rammed earth panel followed by 4in XPS insulation, 4in cavity and 12in rammed earth wall. The centrally located insulation assembly had 6in rammed earth wall followed by 4in XPS insulation, 4in cavity and 10in external rammed earth wall. The external assembly is listed in Table 3. All three insulated assemblies had the same thermal conductivity value.

Table 3 Simulation Model Parameters - Variable Inputs

Layer (Interior to Exterior)	Thickness (inches)	Conductivity (BTU/h·ft·°F)
Uninsulated Rammed Earth (URE 12 in)	12 in (30 cm)	0.417 (0.721 W/m-°K)
Uninsulated Rammed Earth (URE 18 in)	18 in (45 cm)	0.278 (0.481 W/m-°K)
Insulated Rammed Earth (IRE) – 12 in RE, 4 in Cavity, 4 in XPS ,4 in RE	24 in (60 cm)	0.045 (0.077 W/m-°K)
Insulated Wood Frame (IWF) – 0.75 in Stucco, 0.625 in Gypsum Board, 2.6 in R-11 Fiber Glass Batt Insulation, 4 in Wood Framing	5.375 in (13.652 cm)	0.094 (0.163 W/m-°K)
Brick Cavity Construction (BC) – 4 in Brickwork, 2 in Cavity, 4 in Brickwork, 0.5 in Plaster	8.500 in (21.590 cm)	0.275 (0.476 W/m-°K)
Insulated Concrete (IC) – 8 in Concrete, 2.6 in R-11 Fiber Board Insulation, 0.5 in Gypsum Board	11.100 in (28.194 cm)	0.076 (0.131 W/m-°K)

RESULTS AND DISCUSSION

The results were initially used to investigate the best rammed earth wall thickness and insulation location that were then implemented in the comparative analysis with the conventional assemblies.

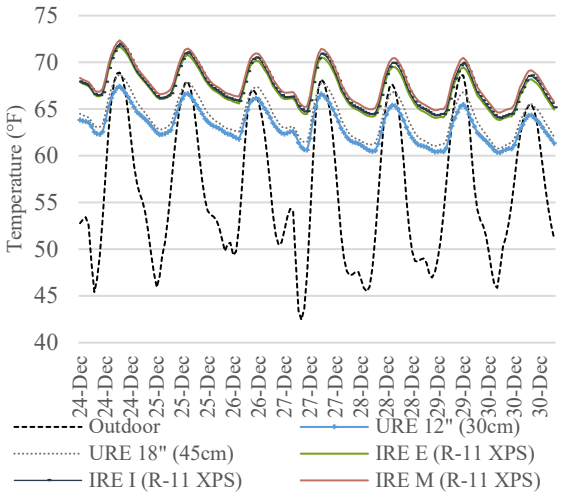

Figure 2 Comparison of indoor air temperature for winter design week for Jaipur, India showing impact of insulation location and thickness of rammed earth assemblies

URE 12" – Uninsulated Rammed Earth 12in thick; URE 18" Uninsulated Rammed Earth 18in thick; IRE E – Semi-externally Insulated Rammed Earth; IRE I – Internally Insulated Rammed Earth; IRE M – Rammed Earth with Central Insulation

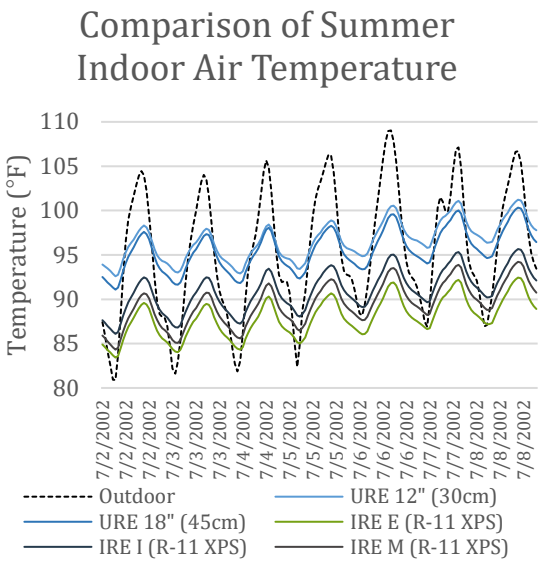

Figure 3 Comparison of indoor air temperature for summer design week for Jaipur, India showing impact of insulation location and thickness of rammed earth assemblies

URE 12" – Uninsulated Rammed Earth 12in thick; URE 18" Uninsulated Rammed Earth 18inthick; IRE E – Semi-externally Insulated Rammed Earth; IRE I – Internally Insulated Rammed Earth; IRE M – Rammed Earth with Central Insulation

As seen in Figure 2 and Figure 3, the insulated rammed earth assemblies outperform the uninsulated assembles for Jaipur (India). Specifically, the semi-externally insulated assembly is shown to perform best by both moderating the temperature fluxes and providing the best indoor comfort condition.

Specifically, the rammed earth assembly with insulation located in the center of the wall section provides better indoor comfort conditions in heating mode, as shown in Figure 2. Additionally, when moving the insulation layer to the exterior of the section (indicated as a "semi-externally insulated rammed earth"), an improved performance is achieved in a cooling mode, as shown in Figure 3. This behavior is shown to provide a tradeoff on an annual basis where the semi-externally insulated rammed earth assembly results in the lowest annual heating and cooling loads, as seen in Figure 4. This is assumingly due to the longer cooling period in hot-arid climates. An annual heating and cooling loads reduction of 45% are achieved by adding external insulation to the 12 inch (30 cm) thick uninsulated rammed earth wall. Overall, the externally insulated assembly resulted in a 6% annual loads reduction, when compared to the assembly with the insulation in the center of the wall section (which is the current common practice in the industry).

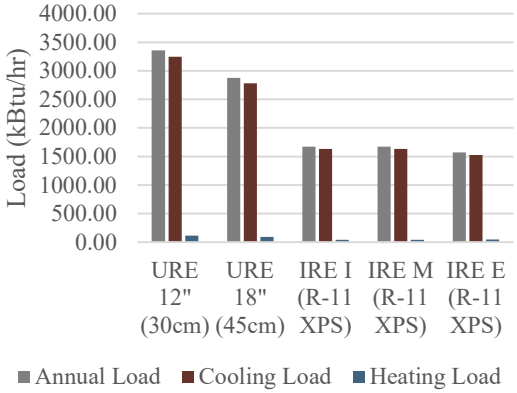

Figure 4 Comparison of annual loads for heating and cooling showing impact of location of insulation within assembly and thickness of thermal mass.

URE 12" – Uninsulated Rammed Earth 12in thick; URE 18" Uninsulated Rammed Earth 18in thick; IRE E – Semi-externally Insulated Rammed Earth; IRE I – Internally Insulated Rammed Earth; IRE M – Rammed Earth with Central Insulation

Further analysis was carried out using the semi-externally insulated rammed earth assembly that was shown to provide the best operational heating and cooling energy loads performance. The additional analysis is conducted to compare the semi-externally insulated rammed earth assembly with conventional building assemblies for the four selected cities as mentions in Table 1.

The comparative results are presented using internal surface temperature fluctuations and indoor air temperatures. The internal surface fluctuations are especially useful in isolating the effects of the wall assemblies' performance and provide an indicative insight into the peak moderating and thermal delay properties of the assemblies.

As seen in Figure 5 and Figure 6, the semi-externally insulated rammed earth assembly can moderate the internal temperatures and therefore reduce heating and cooling consumption when compared to conventional assemblies. This can be noted more prominently in both Figure 7 and Figure 8 that show that the average indoor air temperature fluctuation is only 33% of the outdoor dry bulb temperature fluctuation in summer and 33% in winter when using insulated rammed earth. This is considerable when compared to insulated wood frame which results in an average flux of 79% compared to outdoor temperature variation in summer design week 82% for winter design week.

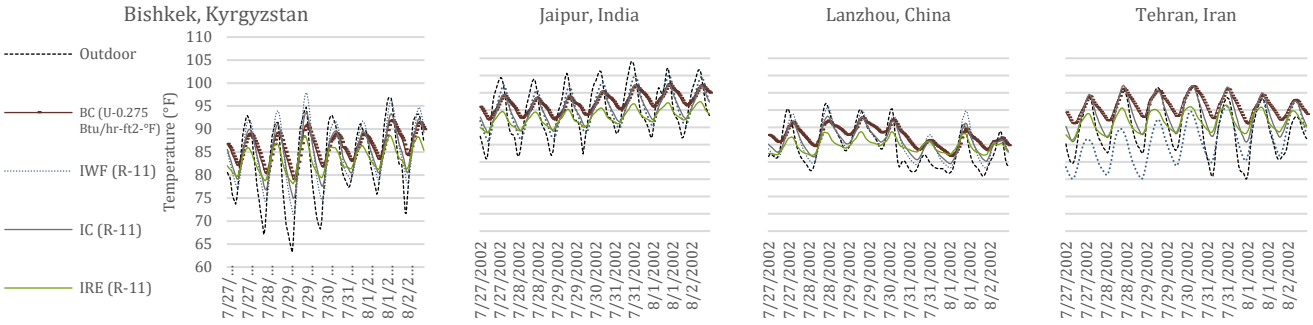

Figure 5 Comparison of Indoor Air Temperatures with Outdoor Temperature for Summer Design Week

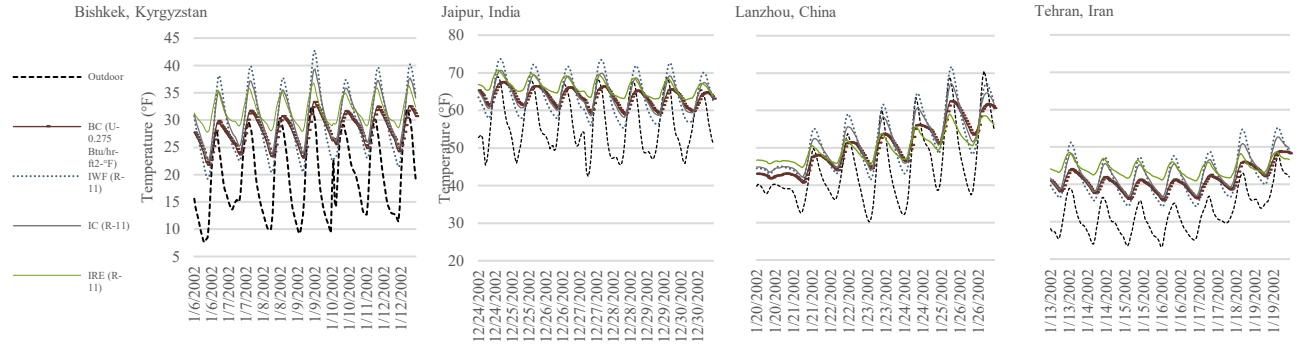

Figure 6 Comparison of Indoor Air Temperatures with Outdoor Temperature for Winter Design Week
BC – Brick Cavity Wall; IWF – Insulated Wood Frame Assembly; IC – Insulated Concrete Assembly; IRE – Insulated Rammed Earth Assembly with Semi-external Insulation

As is further evident from the Figure 5 and Figure 6, the semi-externally insulated rammed earth assembly drives the internal air temperature closest to the setpoint comfort conditions, as prescribed by ASHRAE 55-2010 (ASHRAE, 2010) in both summer and winter. For example, during the summer design week in Jaipur, as shown in Figure 6, the assembly maintains an average temperature of 92.9 °F (33.9 °C) with a high of 97.5 °F (36.4 °C) and minimum of 88.4 °F (31.3 °C) as opposed to a high of 109 °F (42. 8 °C) and low of 81.0 °F (27.2 °C) on the outside. In comparison, a wood frame assembly with similar insulation (R-11) drives the indoor temperature to a high of 105 °F (40.6 °C) and low of 86.0 °F (30.0 °C). This is further illustrated in Figure 9 and Figure 10.

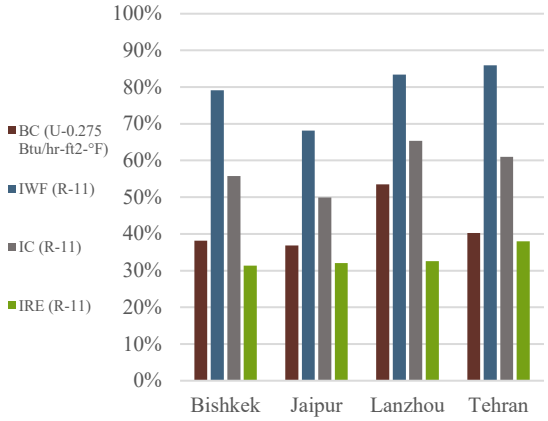

Figure 7 Indoor temperature flux as percentage of outdoor temperature variation for summer design week
BC – Brick Cavity Wall; IWF – Insulated Wood Frame Assembly; IC – Insulated Concrete Assembly; IRE – Insulated Rammed Earth assembly with Semi-external Insulation

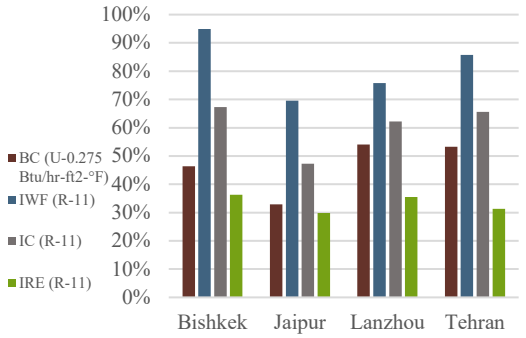

Figure 8 Indoor temperature flux as percentage of outdoor temperature variation for winter design week
BC – Brick Cavity Wall; IWF – Insulated Wood Frame Assembly; IC – Insulated Concrete Assembly; IRE – Insulated Rammed Earth assembly with Semi-external Insulation

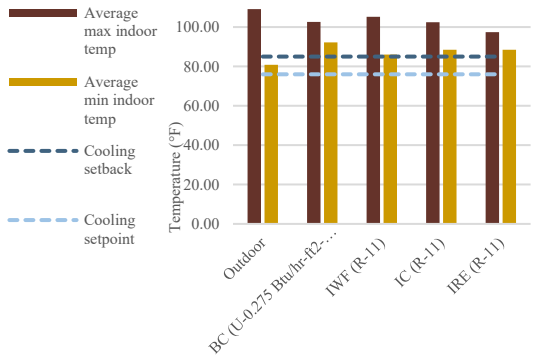

Figure 9 Comparison of indoor air temperature extremes with comfort conditions for summer design week for Jaipur
BC – Brick Cavity Wall; IWF – Insulated Wood Frame Assembly; IC – Insulated Concrete Assembly; IRE – Insulated Rammed Earth assembly with Semi-external Insulation

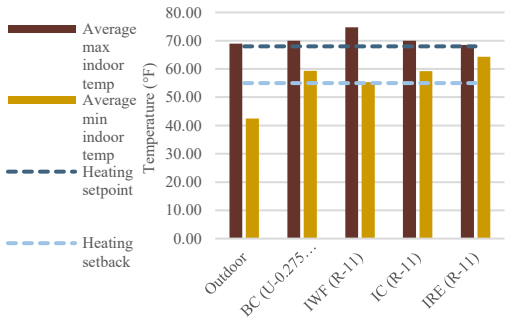

Figure 10 Comparison of indoor air temperature extremes with comfort conditions for winter design week in Jaipur, India
BC – Brick Cavity Wall; IWF – Insulated Wood Frame Assembly; IC – Insulated Concrete Assembly; IRE – Insulated Rammed Earth assembly with Semi-external Insulation

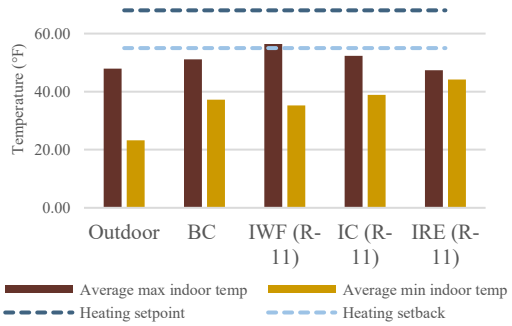

Figure 11 Comparison of indoor air temperature extremes with comfort conditFions for winter design week in Tehran, Iran
BC – Brick Cavity Wall; IWF – Insulated Wood Frame Assembly; IC – Insulated Concrete Assembly; IRE – Insulated Rammed Earth assembly with Semi-external Insulation

As shown in Figure 11., in the milder climate represented by Tehran, the insulated wood frame achieves the highest temperature level in winter but also reaches as low as 35.5 °F (1.9 °C). The average indoor temperature with insulated wood frame is 43.6 °F (6.5 °C) while for insulated rammed earth, it is 45.6 °F (7.5 °C) therefore providing higher thermal comfort.

A comparison of the internal surface temperature fluctuations was assessed in order to analyze the heat transfer through the wall assemblies. It was found that the brick cavity construction and insulated rammed earth have the lowest temperature fluctuations on the internal surface. This helps in moderating the indoor air temperature thereby maintaining the highest radiant comfort.

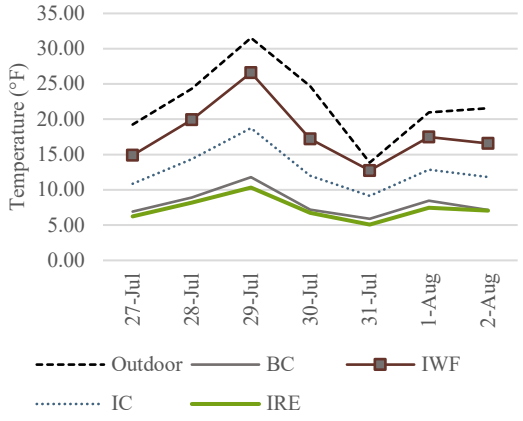

Figure 12 Comparison of Inside Surface Temperature Fluctuation with Outdoor Temperature Fluctuation for Summer Design Week in Bishkek, Kyrgyzstan
BC – Brick Cavity Wall; IWF – Insulated Wood Frame Assembly; IC – Insulated Concrete Assembly; IRE – Insulated Rammed Earth assembly with Semi-external Insulation

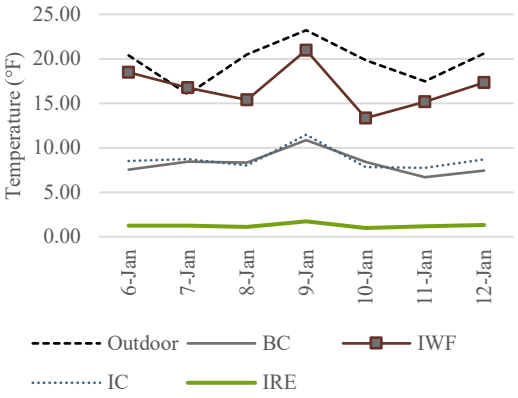

Figure 13 Comparison of Inside Surface Temperature Fluctuation with Outdoor Temperature Fluctuation for Winter Design Week in Bishkek, Kyrgyzstan

BC – Brick Cavity Wall, IWF – Insulated Wood Frame Assembly; IC – Insulated Concrete Assembly; IRE – Insulated Rammed Earth; Assembly with Semi-external Insulation

A similar trend of reduced temperature fluctuations by the rammed earth assembly is seen for all cities, as shown in Figure 12 and Figure 13. The temperature flux on the inside surface is an average of 7.3 °F (4.0 °C) in the summer design week and 1.3 °F (0.7 °C) in winter design week for insulated rammed earth assembly as compared to an average of 17.9 °F (9.9 °C) and 16.8 °F (9.3 °C) respectively for insulated wood frame. Overall, an average of 20% reduction was observed in insulated rammed earth construction as compared to insulated concrete walls. Furthermore, Figure 12 shows that the insulated wood frame assembly has the highest heat transfer within the assembly with internal surface temperatures closely following the outdoor temperature variation. This is further reflected in the annual heating and cooling load calculation shown in Figure 14.

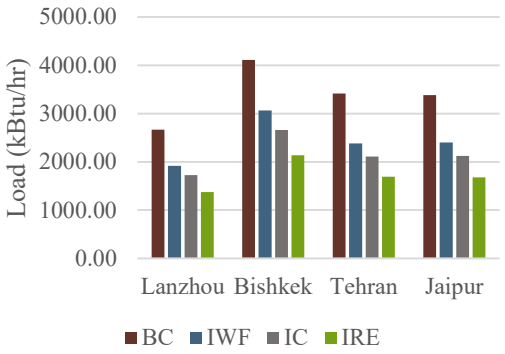

Figure 14 Comparison of annual heating and cooling load for all four assemblies for the simulated cities

BC – Brick Cavity Wall; IWF – Insulated Wood Frame Assembly; IC – Insulated Concrete Assembly; IRE – Insulated Rammed Earth assembly with Semi-external Insulation

CONCLUSION

Rammed earth is a low-carbon, minimally processed, and nontoxic alternative to prevalent construction materials such as concrete and insulated timber frame.

The objective of the study was to investigate the comparative performance of rammed earth assembly as opposed to mainstream construction and the optimum location of insulation. Using dynamic whole-building simulations in hot-arid climates, this study accounts for not only thermal resistance but also the specific heat capacity and therefore testing the implications of both insulation and thermal mass on heating and cooling loads. The results of this study show that insulated rammed earth walls are better suited for hot arid climates than uninsulated rammed earth. It was found that adding insulation to rammed earth wall can reduce the heating and cooling load by 45%. Compared to the common practice of adding insulation in the middle, shifting it towards the exterior can result in an additional 6% reduction.

When compared to conventional assemblies – cavity brick construction, insulated wood frame, and insulated concrete, semi-externally insulated rammed earth outperformed the conventional assemblies in terms of heating and cooling loads reductions, while providing steady indoor comfort temperature levels. Rammed earth assembly had the least inside surface temperature fluctuations, providing an even moderation of indoor air temperature.

When compared to concrete, an average reduction of 18% in annual heating load and 24% in annual cooling load was observed across all modeled cities. Significantly, insulated rammed earth assemblies were shown to reduce residential heating and cooling loads by 20% when compared to insulated concrete walls. These results confirm that in regions with high diurnal variation, thermal mass assemblies can provide better indoor environmental quality through temperature modulation.

While this study compares mainstream assemblies with varied thicknesses, construction costs, and thermal properties, future research should provide an extended systematic comparison while keeping constant thermal and costs constraints. Additionally, a next phase simulation should include the effects of hygrothermal properties in the calculation in order to investigate the impacts of indoor humidity levels.

REFERENCES

Allinson, D., & Hall, M. (2010). Hygrothermal analysis of a stabilised rammed earth test building in the UK. *Energy and Buildings*, 854-852.

Amos-Abanyie, S., & Akuffo, F. K.-S. (2013). Effects of Thermal Mass, Window Size, and Night-Time Ventilation on Peak Indoor Air Temperature in the Warm-Humid Climate of Ghana. *The Scientific World*.

ASHRAE. (2010). ANSI/ASHRAE/IES Standard 55-2010: Energy Standard for Buildings except Low-Rise. Atlanta.

Beck, H., Zimmermann, N., McVicar, T., Vergopolan, N., Berg, A., & Wood, E. (2018). Present and future Köppen-Geiger climate classification maps at 1-km resolution. *Sci Data*. doi:10.1038/sdata.2018.214, 5:180214

Beckett, C., Cardell-Oliver, R., Ciancio, D., & Huebner, C. (2017). Measured and simulated thermal behaviour in rammed earth houses in a hot-arid climate. Part B: Comfort. *Journal of Building Energy*, 146-158.

Blondeau, p., Sperandio, M., & Allard, F. (1997). Night ventilation for building cooling in summer. *Solar Energy*, 327-335.

Cabeza, L. F., Barreneche, C., Miro, L., Morera, J. M., Bartoli, E., & Fernandez, A. (2013). Low carbon and low embodied energy materials in buildings: A review. *Renewable and Sustainable Energy Reviews*, 536-542.

CSIRO. (2000). *Mud walls give poor insulation: CSIRO.* Retrieved from www.dbce.csiro.au/inno-web/0600/mud-walls.htm

DesignBuilder. (2019). DesignBuilder Simulation Version 6.1.2.9.

Dong, X., Soebarto, V., & Griffith, M. (2014). Achieving thermal comfort in naturally ventilated rammed earth houses. *Building and Environment*, 588-598.

Energy, U. D. (2019). EnergyPlus Version 9.2.0.

EnergyPlus. (n.d.). *Engineering Reference - The Reference to EnergyPlus Calculations.* Retrieved 02 2019, from EnergyPlus: https://energyplus.net/sites/default/files/pdfs_v8.3.0/EngineeringReference.pdf

Fodde, E. (2009). Traditional Earthen Building Techniques in Central Asia. *International Journal of Architectural*, 145-168.

Ghattas, R., Ulm, F.-J., & Ledwith, A. (2013). mapping thermal mass benefit. *Concrete sustainability hub*.

Gilly, D. (1787). *Handbuch der Land-Bau-Kunst: vorzüglich in Rücksicht auf die Construction der Wohn- und Wirthschafts-Gebäude für angehende Kameral-Baumeister u. Ökonomen.* Braunschweig and Halle.

Hall, M., & Djerbib, Y. (2006). Moisture ingress in rammed earth:Part 3 – Sorptivity, surface receptiveness and surface inflow velocity. *Construction and Building Materials*, 384–395.

Hugo, H., & Guillaud, H. (1984). Earth Construction Primer. *Craterre, 8*.

Kneifel, J. (2012). *Prototype Residential Building Designs for Energy and Sustainability Assessment.* National Institute of Standards and Technology.

Li, Z., Wang, X., Sun, M., Chen, W., Guo, Q., & Zhang, H. (2011). Conservation of Jiaohe ancient earthen site in China. *Journal of Rock Mechanics and Geotechnical Engineering*, 270-281.

Minke, G. (2006). *Building with Earth: Design and Technology of a Sustainable Architecture.* Basel: Birkhäuser.

Perez-Lombard, L., Ortiz, J., & Pout, C. (2008). A review on buildings energy consumption information. *Energy and Buildings*, 394-398.

Rathore, M., Sharma, S. K., & Preet, V. (2018). Analysis of Traditional and Existing Construction Practices for Sustainable Rural Houses in the Southern Western Part of Rajasthan. *International Journal of Engineering Research & Technology*.

Rubel, F., & Kottek, M. (2004). Observed and projected climate shifts 1901–2100 depicted by world maps of the Koppen-Geiger climate classification. *Meteorologische Zeitschrif*, 135-141.

Ruud, M., Mitchell, J., & Klein, S. (1990). Use of builsing thermal mass to offset cooling loads. *ASHRAE Transactions*.

Sabzi, M. Z. (2018). Survey and Analysis of Various Domes in the Structure of Traditional Iranian Buildings. *Kerpic'18 – Back to Earthen Architecture: Industrialized, Injected, Rammed, Stabilized*, 305-312.

Soudani, L., Woloszyn, M., Fabbri, A., Morel, J.-C., & Grillet, A. (2017). Energy evaluation of rammed earth walls using long term in-situ measurements. *Solar Energy*, 70–80. doi:10.1016/j.solener.2016.11.002

Taylor, P., & Luther, M. (2004). Evaluating rammed earth walls: a case study. *Solar Energy*, 79-84.

Treloar, G. J., Owen, C., & Fay, R. (2001). Environmental assessment of rammed earth construction systems. *Structural Survey*, 99-106.

UN Environmental amnd International Energy Agency. (2017). *Towards a zero-emission, efficient, and resilient buildings and construction sector. Global Status Report 2017.*

Uranova, S., & Begaliev, U. T. (2002). *World Housing Encyclopedia: an Encyclopedia of Housing Construction in Seismically Active Areas of the World.* Earthquake Engineering Research Institute; International Association for Earthquake Engineering.

Wilcox, S., & Marion, W. (2008). Innovation for Our Energy Future Users Manual for TMY3 Data Sets. Retrieved from http://www.osti.gov/bridge